Estimating phase synchronization in dynamical systems using cellular nonlinear networks

Robert Sowa,[1,2] Anton Chernihovskyi,[1,2] Florian Mormann,[1] and Klaus Lehnertz[1,2,*]
[1]*Department of Epileptology, Neurophysics Group, University of Bonn, Sigmund-Freud-Strasse 25, D-53105 Bonn, Germany*
[2]*Helmholtz-Institute for Radiation and Nuclear Physics, University of Bonn, Nussallee 14-16, 53115 Bonn, Germany*
(Received 19 November 2004; published 29 June 2005)

We propose a method for estimating phase synchronization between time series using the parallel computing architecture of cellular nonlinear networks (CNN's). Applying this method to time series of coupled nonlinear model systems and to electroencephalographic time series from epilepsy patients, we show that an accurate approximation of the mean phase coherence R—a bivariate measure for phase synchronization—can be achieved with CNN's using polynomial-type templates.

DOI: 10.1103/PhysRevE.71.061926 PACS number(s): 87.19.La, 05.10.−a, 05.45.Tp, 07.05.Mh

I. INTRODUCTION

Artificial neural networks (ANN's) are computational tools that have found extensive utilization in solving complex real-world problems. The attractiveness of ANN's comes from their information-processing characteristics such as intrinsic nonlinearity, high parallelism, and fault and noise tolerance. More importantly, neural networks are able to learn a rule from a set of examples [1] and, after successful supervised or unsupervised learning, are capable of generalization. For more than a decade ANN's have been used to model, to generate, and to predict time series, including chaotic ones (see, e.g., [2–9]). Only a few studies [10–13], however, report on the use of neural networks to directly estimate characterizing measures from time series.

Since a conventional (i.e., von Neumann) computer architecture is not well suited to simulate large-scale neural networks, there is need for a special parallel architecture (that even allows mobile field applications). CNN is an acronym for either *cellular neural network* when used in the context of brain sciences or *cellular nonlinear network* when used in the context of coupled dynamical systems [14,15]. In this paper we shall use the acronym CNN with the latter meaning. The concept of CNN was developed in 1988 by Chua and Yang [16,17]. The general idea was to combine the architecture of cellular automata and neural networks. Simply speaking, a CNN is an array of locally coupled nonlinear electrical circuits or cells which is capable to process a large amount of information in parallel and in real time. Interactions between the cells of a CNN are only local and usually translation invariant; i.e., a connection from a cell j toward another cell i only exists if j is part of i's neighborhood $\mathcal{U}(i)$ and its type and strength depend only on the relative position of j with respect to i. Thus the number of connections increases only linearly with the number of cells, a property that enables hardware realization of CNN [e.g., very-large-scale integrated implementations (VLSI)], as opposed to other types of ANN's.

Processing of information with a dynamical system—such as CNN—can be considered as an evolution of its initial state to some desired final state which is regarded as the result of computation. A CNN is thus *programmed* by defining an appropriate interaction pattern (i.e., a connection *template* between cells), an initial state, and boundary conditions. A number of different approaches have been exploited in the past to study CNN dynamics (see [18] for an overview). Apart from software simulators that are based on the numerical integration of a set of ordinary differential equations, these approaches include digital and mixed digital and analog (so-called *analogic*) CNN. A digital CNN consists of an array of standard digital signal processors or of special-purpose processors combined with digital memory units. An analogic CNN consists of an array of analog processing units, has both analog and digital memory units, and has already been realized in VLSI [15]. In contrast to digital CNN's, analogic CNN implementations provide a much higher computational performance under equivalent energy and size requirements. However, the operational range of the analog circuitry as well as the low tolerance against parameter fluctuations restricts the applicability of analogic CNN and requires a more detailed analysis of the stability of network dynamics. Since both digital and analogic CNN's possess memory units, these architectures allow one to realize *stored programmability*, which is an essential feature of universal computation [18]. Thus the CNN paradigm is a universal Turing machine [so-called CNN universal machine (CNN-UM)] and therefore includes cellular automata as a special case. Due to an intrinsic nonlinearity, a variety of complex phenomena can be simulated on a CNN (e.g., self-organization, dissipative structures, or chaos; see [15,19] for an overview).

Synchronization phenomena in dynamical systems have attracted much attention in various scientific fields ranging from physics to the neurosciences (see [20] for an overview). Different frameworks for the mathematical description of synchronization have been developed which have led to the proposition of different concepts of synchronization. Among others, the classical concept of phase synchronization was extended from linear to nonlinear or even chaotic systems for cases where the definition of a phase variable is possible for the analyzed systems [21].

One of the most challenging dynamical systems in nature is the human brain. Constituted by a complex network of a huge number of neurons, which introduce nonlinearity to the system even on a cellular level, the dynamics of this system has long been a focus of (mostly univariate) linear and non-

*Electronic address: klaus.lehnertz@ukb.uni-bonn.de

linear time series analysis [22–26]. A malfunction of the brain that is known to be particularly associated with a pathological neuronal synchronization is the disease epilepsy along with its cardinal symptom, the epileptic seizure. Led by a growing interest in the possibility of seizure prediction (see [27] for an overview), a number of analysis techniques have been proposed. It is only recently that bivariate analysis techniques were repeatedly shown to contribute significantly to this field.

Following the approach of understanding phase synchronization in a statistical sense [28], we have developed a straightforward measure for phase synchronization employing the circular variance of a phase distribution. We have termed this measure *mean phase coherence R* (see [29,30] and references therein). In this approach, the phase variable is obtained from the Hilbert transform of an electroencephalographic (EEG) signal. Recent studies [31,32] show that a long-lasting (up to hours) preseizure state can be defined from the temporal evolution of R, which consists of shifts in synchronization that deviate significantly from the levels observed during the seizure-free interval. The sensitivity and specificity of this bivariate analysis technique outperform previously used univariate analysis techniques and appears to be promising for prospective clinical studies [33].

Despite its conceptual simplicity (estimation of R between two time series mainly requires a forward and an inverse fast Fourier transform), the required computational resources grow quadratically with the number of channels to be analyzed. This limits real-time applications (e.g., in clinical or neuroscientific settings) to a certain extent. A more efficient data analysis demands the parallel processing power of ANN's. In this study we show that cellular nonlinear networks allow a sufficiently accurate approximation of the degree of phase synchronization between two time series. After a successful optimization of the network, our approach can in principle be used for the analysis of multichannel data.

This article is organized as follows. In Sec. II A we briefly recall the definitions for phase synchronization and for the mean phase coherence R. The methods used to approximate R with a cellular nonlinear network are presented in Sec. II B. In Sec. III we show the results of our application to time series from model systems and to EEG time series from epilepsy patients, before we draw our conclusions in Sec. IV.

II. METHODS

A. Measuring phase synchronization

Traditionally, phase synchronization is defined as the locking of the phases ϕ of two oscillating systems a and b [34]:

$$\phi_a(t) - \phi_b(t) = \text{const}. \tag{1}$$

As a measure to quantify the degree of phase synchronization between two time series, we used the *mean phase coherence R* [29,30] defined as

$$R = \left| \frac{1}{K} \sum_{j=0}^{K} e^{i[\phi_a(j\Delta t) - \phi_b(j\Delta t)]} \right| = 1 - V, \tag{2}$$

where $1/\Delta t$ is the sampling rate of the discrete time series of length K and V denotes the circular variance of an angular distribution obtained by transforming the differences in phase onto the unit circle in the complex plane [35]. By definition, R is confined to the interval [0,1] where $R=1$ ($V=0$) indicates fully synchronized systems.

In order to determine the phases $\phi_a(t)$ and $\phi_b(t)$ of two signals $s_a(t)$ and $s_b(t)$, we followed the analytic signal approach which renders an unambiguous definition of the so-called instantaneous phase for an arbitrary signal $s(t)$:

$$\phi(t) = \arctan \frac{\tilde{s}(t)}{s(t)}, \tag{3}$$

where

$$\tilde{s}(t) = \frac{1}{\pi} \mathrm{p} \int_{-\infty}^{+\infty} \frac{s(\tau)}{t-\tau} d\tau \tag{4}$$

is the Hilbert transform of the signal ("p" denoting the Cauchy principal value). Application of the convolution theorem turns the last equation into

$$\tilde{s}(t) = -i\mathcal{F}^{-1}[\mathcal{F}[s(t)]\mathrm{sgn}(\omega)], \tag{5}$$

where $\mathcal{F}$ denotes Fourier transformation and $\mathcal{F}^{-1}$ inverse Fourier transformation, respectively.

For the analyses presented in Sec. III we performed three steps of data preprocessing for each data window prior to the calculation of the mean phase coherence R. First, the data of each window were normalized to zero mean, which corresponds to setting the dc Fourier coefficient to zero. Second, to avoid edge effects, each window was tapered using a cosine half-wave (Hanning window) before performing the Fourier transform. Third, since the calculation of the Hilbert transform requires integration over infinite time, which cannot be performed for a window of finite length, 10% of the calculated instantaneous phase values are discarded on each side of every window.

B. Estimating phase synchronization with cellular nonlinear networks

1. General considerations

According to Ref. [15] a CNN is any spatial arrangement of locally coupled cells, where each cell is a dynamical system which has an input, an output, and a state evolving according to some prescribed dynamical law. We here consider a CNN which consists of a two-dimensional $M \times N$ homogeneous lattice of cells with local nonlinear interactions. The corresponding state equation for cell (i,j) reads

$$\frac{d}{d\tau}x_{i,j}(\tau) = -x_{i,j}(\tau) + \sum_{k,l\in\mathcal{U}_A} A_{k,l}(y_{i-k,j-l}(\tau)) + \sum_{k,l\in\mathcal{U}_B} B_{k,l}(u_{i-k,j-l}) + Z, \quad (6)$$

where $x_{i,j}(\tau)$ denotes the state variable of cell (i,j) and $y_{k,l}(\tau)$ the output variable of cell (k,l) according to

$$y_{k,l}(\tau) = f(x_{k,l}(\tau)) = \frac{2}{1+e^{-4x_{k,l}(\tau)}} - 1, \quad (7)$$

given an external input variable $u_{k,l}$ as well as feedback and feed-forward template functions $A_{k,l}$ and $B_{k,l}$ (with spheres of influence $k,l\in\mathcal{U}_A$ or $\in\mathcal{U}_B$), respectively. Z denotes a global cell bias. While template function A operates on the outputs of cell (k,l), the template function B operates on the external inputs in the neighborhood of cell (k,l). Both templates and the cell bias Z have to be determined (e.g., by some learning algorithm) to achieve the desired CNN behavior.

2. Network optimization and learning procedures

In order to determine an appropriate CNN with cell outputs showing the behavior of the mean phase coherence R, we performed all simulations using SCNN, a full feature simulation system [36]. First, the basic CNN structure had to be determined, which included the network arrangement, the neighborhood size $\mathcal{U}$, the weight functions $A_{k,l}$ and $B_{k,l}$, and the output function $y_{k,l}(\tau)$.

For the given time series length K of 4096 data points (see Sec. III), we restricted ourselves to a 64×64 network arrangement with a minimum possible 3×3 neighborhood size. We tested different polynomial-type template functions

$$A_{k,l}^{(P)}(z) = \sum_{p=1}^{P} a_{k,l}^{(p)} z^p, \quad (8)$$

$$B_{k,l}^{(Q)}(z) = \sum_{q=1}^{Q} b_{k,l}^{(q)} z^q, \quad (9)$$

of order P and Q (with $P=Q\in[1,4]$), as well as different boundary conditions. Highest performance was achieved for polynomial template functions of order $P=Q=2$ and for the so-called *closed spiral* boundary condition where all boundary cells are connected to the other side of the network, but the connection has an offset of 1 for each row.

Second, in order to present the time series to the network, we followed Ref. [11] and used a linewise alignment (i.e., the rightmost cell in a row is connected to the leftmost cell in the following row) of the windowed time series, where time series $s_a(n)$, $n=1,\ldots,K$, was assigned to the input u and $s_b(n)$ to the state $x(0)$ of the CNN.

Third, in order to train the network we randomly selected L representative pairs of time series (see Sec. III) along with their corresponding values of the mean phase coherence R (see Sec. II A). Half of these values were taken from the interval $R_{\text{low}}\in[0.25,0.35]$ and the other half from the interval $R_{\text{high}}\in[0.85,0.95]$. The desired output y^{Ref} was set to $+1$ for R_{high} and to -1 for R_{low}. After choosing random initial values for the components of templates A and B and for the global cell bias Z, the following cost function was minimized iteratively using the method of simulated annealing [37]:

$$\Gamma = \frac{1}{L}\sum_{l=1}^{L}\left(\frac{1}{4K}\sum_{n=0}^{N-1}[y_{l,n}(\tau_{\text{trans}}) - y_{l,n}^{\text{Ref}}]^2\right). \quad (10)$$

This cost function can be interpreted as the *energy* E of a thermodynamic system, which is annealed slowly toward the global minimum. In each iteration step, Γ is updated and depending on the present *temperature* T this exchange is accepted with probability

$$p(\Delta E,T) = \begin{cases} e^{-\Delta E/T}, & \Delta E > 0, \\ 1, & \Delta E \leqslant 0. \end{cases} \quad (11)$$

Exchanges with increasing energy are also accepted with nonzero probability to allow escaping from local minima. In our applications we started at an initial *temperature* of $T_0=50$, allowed for 300 cooling steps, and assigned Γ the minimum value found after a total of 15 000 iteration steps. Note that Eq. (10) evaluates all L desired outputs for each iteration step.

Other minimization procedures (e.g., Powell's or downhill simplex [38]) were tested, but did not lead to comparably accurate results. Following Ref. [10] the training was performed not up to a steady state [i.e., $y(\tau)\Rightarrow y(\infty)$], but up to some fixed transient time τ_{trans}. For this purpose we integrated Eq. (6) using Euler's method with a step size of $h=0.2$ and 200 integration steps resulting in a transient time $\tau_{\text{trans}}=40$. Other integration schemes were tested, but did not lead to further improvements of accuracy. The approximated mean phase coherence R^{CNN} is defined as

$$R^{\text{CNN}} = \left(\frac{1}{K}\sum_{k=0}^{K-1}\frac{y_k(\tau_{\text{trans}})+1}{2}\right)(R_{\max}-R_{\min}) + R_{\min}, \quad (12)$$

where $R_{\min}$ and $R_{\max}$ can be chosen either as 0 and 1 or as >0 and <1, respectively, depending on the specific application (see Sec. III).

III. APPLICATIONS

A. Model systems

We studied two diffusively coupled Rössler systems (cf. [39]):

$$\dot{x}_{1,2} = -\omega_{1,2}y_{1,2} - z_{1,2} + \epsilon(x_{2,1} - x_{1,2}),$$

$$\dot{y}_{1,2} = \omega_{1,2}x_{1,2} + 0.165y_{1,2},$$

$$\dot{z}_{1,2} = 0.2 + z_{1,2}(x_{1,2} - 10), \quad (13)$$

with a mismatch of the natural frequencies $\omega_1=0.89$ and $\omega_2=0.85$. The coupling is introduced in the last term of the first equation, where ϵ denotes the coupling strength. The differential equations were iterated using a fourth-order Runge-Kutta algorithm [38] with a step size of 0.1. In order to eliminate transients, the first 10^3 iterations were discarded. For $\epsilon\in\{0.00,0.01,0.02,0.03,0.04\}$ we generated scalar time

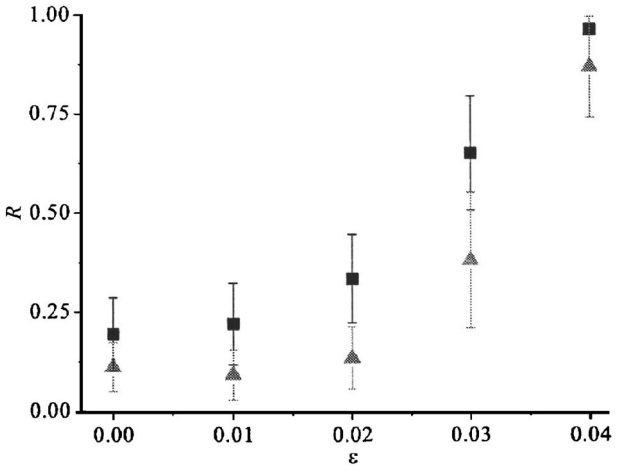

FIG. 1. Means and standard deviations of calculated (rectangles) and approximated mean phase coherence (triangles) for coupled Rössler systems using different coupling strengths ϵ. (Note that the standard deviation of the calculated mean phase coherence for $\epsilon = 0.04$ is smaller than the chosen symbol size.)

series of the x components each consisting of 116×4096 data points. Time series were split into 116 consecutive overlapping windows of length $K=4096$, where the overlap amounted to 20% in order to account for the preprocessing steps defined in Sec. II A. The mean phase coherence R was then calculated for each of these windows. As *training set*, we randomly selected $L=16$ representative pairs of time series along with their corresponding R values, proceeded as described in Sec. II B 2, and obtained $\Gamma=0.071$.

R^{CNN} values for the *test set*, which consisted of the remaining 100 time series pairs, were then estimated using $R_{\mathrm{min}}=0$ and $R_{\mathrm{max}}=1$ [cf. Eq. (12)]. From the results shown in Fig. 1 it can be seen that the CNN allows one to approximate the mean phase coherence with a sufficient accuracy. Taking into account the rather limited range of R values used for training the CNN and the small number of data points the time series consisted of, we regard the average deviation of 15.5% as sufficiently low, particularly for field applications aiming to differentiate between strongly and only weakly synchronized states. Such an application will be presented in the next section.

B. EEG data

We analyzed quasicontinuous multichannel EEG recorded from an epilepsy patient over 5 days during which the patient had ten epileptic seizures of focal origin. The EEG was measured from electrodes implanted directly within the brain prior to and independently from the design of this study during the presurgical work-up. EEG data were sampled at 200 Hz using a 16-bit analog-to-digital converter and filtered within a frequency band of 0.5–85 Hz. All ten seizures occurred spontaneously within the second half of the recording. We here restrict ourselves to the analysis of EEG data from two sets of pairs (P_1, P_2) of recording channels. Previous studies [33] have shown that the temporal evolution of R calculated for set P_1 exhibited highest seizure prediction performance. Set P_2 was taken from the opposite brain hemisphere (homologous sites) and served to study generalization properties of the CNN. Due to the high amplitude variability of the EEG, we linearly mapped, as an additional preprocessing step, the amplitude range of $[-150, 150]$ mV of the normalized (zero mean) EEG to the CNN range of $[-1, 1]$. R values were then calculated (see Sec. II A) using a moving-window technique with 20% overlapping segments of 20.48 s corresponding to $K=4096$ data points. The number of R values for each set thus amounted to 23417.

As *training set* we randomly selected $L=16$ EEG time series pairs from set P_1 along with their corresponding R values using criteria defined in Sec. II B 2. These time series were taken from the seizure-free interval and from the preseizure period. After minimizing Eq. (10) we achieved $\Gamma=0.089$. The obtained CNN settings were then used to calculate R^{CNN} values for the *test set* which consisted of the remaining 23416 time series pairs from set P_1 using $P_{\mathrm{min}}=0.3$ and $R_{\mathrm{max}}=0.9$ [cf. Eq. (12)]. These values were chosen based on the frequency distribution of all R values calculated for this EEG data set. In Fig. 2 we present the temporal evolutions of R and R^{CNN}.

Despite the extremely small subset of data used to train the network (a recording time of about 330 s only), the overall temporal variability of the mean phase coherence is reproduced with a sufficient quality, the average deviation amounting to 5.2% only. A more detailed analysis of the obtained profiles (data not shown here) revealed that a long-lasting (>60 min) drop in synchronization before the seizure that deviates significantly from the values observed during the seizure-free interval could be observed prior to seven out of the ten seizures. These findings indicate that a differentiation between these states is in principle possible using R^{CNN}, although the achieved performance might not be sufficient for all cases. Nevertheless, it should be noted that the CNN allows a sufficient approximation of R even during and after the seizure, although we did not use data from these states for the training.

In order to study further generalization properties of the network, we used the CNN settings obtained from training the subset of data from set P_1 but calculated R^{CNN} values for the complete set P_2. Figure 3 shows that the overall temporal variability of the mean phase coherence is reproduced even better, the average deviation amounting to 0.08% only. This small error, however, can be in part be attributed to the restricted temporal variability of R found for this set.

IV. CONCLUSION

We have demonstrated the feasibility of cellular nonlinear networks (CNN's) to characterize synchronization phenomena in dynamical systems, based on a pair of measured time series. By applying CNN's to both time series from coupled nonlinear model systems and long-lasting EEG recordings from an epilepsy patient, we have shown that CNN's with polynomial-type template functions allow a sufficiently accurate approximation of the mean phase coherence R, an established measure for phase synchronization in time series analysis.

At present, our findings are restricted to simulated or digital realizations of CNN's, both providing an almost arbitrary

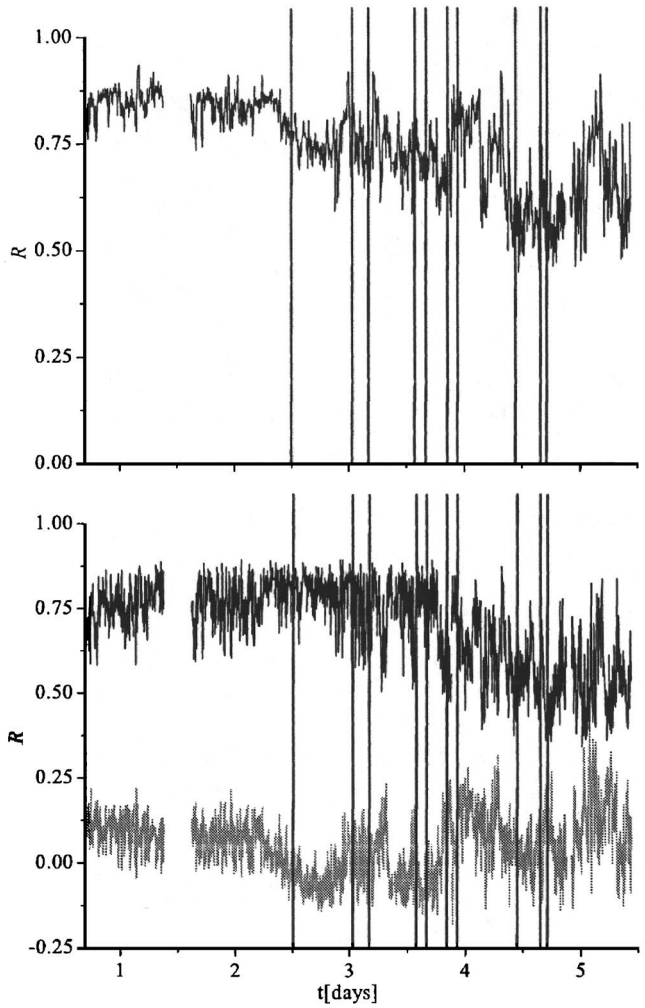

FIG. 2. Calculated (top) and approximated (bottom) mean phase coherence for set P_1. The gray line in the lower part of the figure indicates the point-by-point difference between R and R^{CNN}. Seizures are marked by vertical lines. Profiles are smoothed using a ten-point moving-average filter for better visualization. Twice the patient was briefly (13 and 54 min) disconnected from the EEG acquisition system. A longer discontinuity (340 min) was necessary to carry out a magnetic resonance imaging scan to determine the exact location of the implanted electrodes.

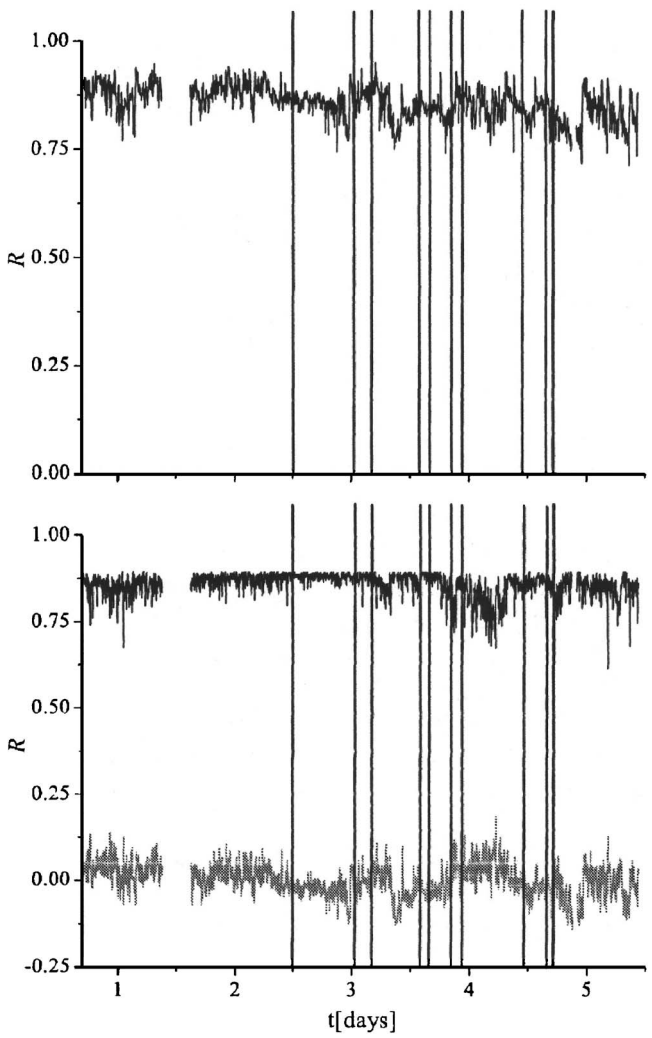

FIG. 3. Same as Figure 2 but for set P_2.

precision. For an implementation on analogic CNN's the limitations of the analog part—i.e., a limited precision and the need for polynomial-type templates—have to be taken into account. Nevertheless, in addition to already existing polynomial-type analog CNN's [40,41], it has been shown that nonlinear templates can well be approximated by piecewise linear functions [42]. Using different optimization strategies, the authors in Refs. 43 and 44 have shown that the templates and the bias of a CNN can be adjusted in such a way that the effect of hardware tolerances is minimized. These optimizations increase tolerance against parameter fluctuations and lead to a more robust behavior of analogic CNN's. More recently, it has been shown that robust templates, which do not only work on CNN simulators, but also on hardware implementations can be found using an on-chip optimization [45]. It can thus be expected that linear or nonlinear templates can be adapted to an existing CNN hardware chip. The question whether these optimization strategies allow an implementation of our phase estimation approach on analogic CNN's will be subjected to further research. Nevertheless, the generalization properties and the high computational performance of CNN's along with the small energy and space requirements render CNN attractive for future VLSI implementations which may even lead to the development of miniaturized analysis systems.

Although the EEG database used in this study was from a single patient, the achieved results can be regarded as promising. Further evaluations on a larger EEG database are currently underway. It would also be interesting to extend this work to other bivariate measures that have been successfully applied to characterize brain dynamics, such as mutual information [46] or nonlinear interdependences [47].

ACKNOWLEDGMENTS

We thank Peter David and Ronald Tetzlaff for close support and for valuable comments on earlier versions of this manuscript. This work was supported by the Deutsche Forschungsgemeinschaft (Grant No. LE 660/2-1).

[1] T. Watkin, A. Rau, and M. Biehl, Rev. Mod. Phys. **65**, 499 (1993).
[2] A. Lapedes and R. Farber (unpublished).
[3] A. M. Albano, A. Passamante, T. Hediger, and M. E. Farrell, Physica D **58**, 1 (1992).
[4] J. Principe, A. Rathie, and J. Kuo, Int. J. Bifurcation Chaos Appl. Sci. Eng. **2**, 989 (1992).
[5] E. Eisenstein, I. Kanter, D. A. Kessler, and W. Kinzel, Phys. Rev. Lett. **74**, 6 (1995).
[6] D. R. Kulkarni, J. C. Parikh, and R. Pratap, Phys. Rev. E **55**, 4508 (1997).
[7] R. Bakker, J. C. Schouten, C. L. Giles, F. Takens, and C. M. van den Bleek, Neural Comput. **12**, 2355 (2000).
[8] A. Freking, W. Kinzel, and I. Kanter, Phys. Rev. E **65**, 050903 (2002).
[9] M. Small and C. Tse, Phys. Rev. E **66**, 066701 (2002).
[10] R. Tetzlaff, R. Kunz, C. Ames, and D. Wolf, in *Proceedings of the IEEE European Conference on Circuit Theory and Design*, edited by C. Beccari, M. Biey, P. P. Civalleri, and M. Gill (Levrotto & Bella, Turin, 1999), p. 1007–1010.
[11] R. Kunz, R. Tetzlaff, and D. Wolf, in *Proceedings of the IEEE International Symposium on Circuits and Systems*, edited by J. Vandevalle and M. Hassler (IEEE, Piscataway, NJ, 2000), p. 1024-1027.
[12] A. Potapov and M. Ali, Phys. Rev. E **65**, 046212 (2002).
[13] R. Kunz and R. Tetzlaff, J. Circuits Syst. Comput. **12**, 825 (2003).
[14] L. O. Chua, Int. J. Bifurcation Chaos Appl. Sci. Eng. **7**, 2219 (1997).
[15] L. O. Chua, *CNN: A paradigm for complexity* (World Scientific, Singapore, 1998).
[16] L. O. Chua and L. Yang, IEEE Trans. Circuits Syst. **35**, 1257 (1988).
[17] L. O. Chua and L. Yang, IEEE Trans. Circuits Syst. **35**, 1273 (1988).
[18] L. O. Chua and T. Roska, *Cellular Neural Networks and Visual Computing* (Cambridge University Press, Cambridge, UK, 2002).
[19] R. Dogaru, *Universality and Emergent Computation in Cellular Neural Networks* (World Scientific, Singapore, 2003).
[20] A. S. Pikovsky, M. G. Rosenblum, and J. Kurths, *Synchronization—A universal concept in nonlinear sciences* (Cambridge University Press, Cambridge, UK, 2001).
[21] M. Rosenblum, A. Pikovsky, and J. Kurths, Phys. Rev. Lett. **76**, 1804 (1996).
[22] E. Başar, *Chaos in Brain Function* (Springer, Berlin, 1990).
[23] D. Duke and W. Pritchard, *Measuring Chaos in the Human Brain* (World Scientific, Singapore, 1991).
[24] B. H. Jansen and M. E. Brandt, *Nonlinear Dynamical Analysis of the EEG* (World Scientific, Singapore, 1993).
[25] K. Lehnertz, J. Arnhold, P. Grassberger, and C. E. Elger, *Chaos in Brain?* (World Scientific, Singapore, 2000).
[26] H. Kantz and T. Schreiber, *Nonlinear Time Series Analysis* (Cambridge University Press, Cambridge, UK, 2003).
[27] B. Litt and K. Lehnertz, Curr. Opin. Neurol. **15**, 173 (2002).
[28] P. Tass, M. Rosenblum, J. Weule, J. Kurths, A. Pikovsky, J. Volkmann, A. Schnitzler, and H. Freund, Phys. Rev. Lett. **81**, 3291 (1998).
[29] M. Hoke, K. Lehnertz, C. Pantev, and B. Lütkenhöner, in *Dynamics of Cognitive and Sensory Processing in the Brain*, edited by E. Başar and T. Bullock (Springer, New York, 1988), pp. 84–105.
[30] F. Mormann, K. Lehnertz, P. David, and C. E. Elger, Physica D **144**, 358 (2000).
[31] F. Mormann, R. G. Andrzejak, T. Kreuz, C. Rieke, P. David, C. E. Elger, and K. Lehnertz, Phys. Rev. E **67**, 021912 (2003).
[32] F. Mormann, T. Kreuz, R. G. Andrzejak, P. David, K. Lehnertz, and C. E. Elger, Epilepsy Res. **53**, 173 (2003).
[33] F. Mormann, T. Kreuz, C. Rieke, R. G. Andrzejak, A. Kraskov, P. David, C. E. Elger, and K. Lehnertz, Clin. Neurophysiol. **116**, 569 (2005).
[34] C. Hugeneii, *Horoloquium Oscilatorum* (Apud F. Muguet, Paris, 1673).
[35] K. V. Mardia, *Probability and Mathematical Statistics: Statistics of directional data* (Academy Press, London, 1972).
[36] R. Kunz, A. Loncar, and R. Tetzlaff, in *Proceedings of the 6th IEEE International Workshop on Cellular Neural Networks and Their Applications*, edited by L. Fortuna (IEEE, Piscataway, NJ, 2000), p. 123-134.
[37] R. V. V. Vidal, *Applied Simulated Annealing. Lecture Notes in Economics and Mathematical Systems* (Springer, New York, 1993), Vol. 396.
[38] W. Press, S. Teukolsky, W. Vetterling, and B. Flannery, *Numerical Recipes in C: The art of scientific computing* (Cambridge University Press, Cambridge, UK, 1992).
[39] M. Rosenblum, A. Pikovsky, and J. Kurths, Phys. Rev. Lett. **78**, 4193 (1997).
[40] M. Laiho, A. Paasio, A. Kananen, and K. Halonen, Int. J. Circuit Theory Appl. **30**, 165 (2002).
[41] M. Laiho, A. Paasio, A. Kananen, and K. Halonen, IEEE T Circuits-I **51**, 286 (2004).
[42] G. Geis, M. Reinisch, R. Tetzlaff, and F. Puffer, in *Proceedings of the 8th IEEE International Workshop on Cellular Neural Networks and their Applications*, edited by T. Roska, M. Gilli, B. Shi, and A. Zarandy (Amulett'98 Kft., Budapest, 2004), pp. 393–398.
[43] R. Tetzlaff, R. Kunz, and D. Wolf, Int. J. Circuit Theory Appl. **27**, 77 (1999).
[44] R. Schönmeyer, D. Feiden, and R. Tetzlaff, in *Proceedings of the 7th IEEE International Workshop on Cellular Neural Networks and their Applications*, edited by R. Tetzlaff (World Scientific, Singapore, 2002), pp. 523–532.
[45] D. Feiden and R. Tetzlaff, Proc. SPIE **5117**, 470 (2003).
[46] M. Palus, V. Komarek, Z. Hrncir, and K. Sterbova, Phys. Rev. E **63**, 046211 (2001).
[47] J. Arnhold, P. Grassberger, K. Lehnertz, and C. E. Elger, Physica D **134**, 419 (1999).